NO reduction by CO under oxidative conditions over CoCuAl mixed oxides derived from hydrotalcite-like compounds: Effect of water

Joudia Akil, Carmen Ciotonea, Stéphane Siffert, Sébastien Royer, Laurence Pirault-Roy, Renaud Cousin, Christophe Poupin

Version of Record: https://www.sciencedirect.com/science/article/pii/S0920586121002248
Manuscript_3dacf9532355ed57627377aaea847b91

NO reduction by CO under oxidative conditions over CoCuAl mixed oxides derived from hydrotalcite-like compounds: Effect of water

Joudia Akil[1], Carmen Ciotonea[2,4], Stéphane Siffert[1], Sébastien Royer[2], Laurence Pirault-Roy[3], Renaud Cousin[1], Christophe Poupin[1]

[1] *Univ. Littoral Côte d'Opale, UR 4492, UCEIV, Unité de Chimie Environnementale et Interactions sur le Vivant, SFR Condorcet FR CNRS 3417, F-59140 Dunkerque, France.*

[2] *Univ. Lille, CNRS, Centrale Lille, Univ. Artois, UMR 8181 – UCCS – Unité de Catalyse et Chimie du Solide, 59000 Lille, France.*

[3] *Institut de chimie des milieux et matériaux de Poitiers (IC2MP), Université de Poitiers, UMR 7285 CNRS, 4, rue Michel Brunet, 86073 Poitiers cedex 9, France.*

[4] *Univ. Lille, CNRS, INRA, Centrale Lille, Univ. Artois, FR 2638 – IMEC – Institut Michel-Eugène Chevreul, 59000 Lille, France.*

Abstract

Oxyfuel combustion is a promising technology to produce CO_2 rich effluents. Nevertheless, storage as well as valorization steps require to increase the purity of these CO_2 rich effluents due to the presence of CO and NO_x produced during combustion process. In view of development of transition metal-based catalyst for this application, cobalt and/or copper derived hydrotalcite materials were used as precursor of oxide catalyst for NO-CO abatement in a gas stream similar to those obtained when an oxyfuel combustion is performed. Hydrotalcite precursors and catalysts were characterized by several techniques. The best catalytic performances for the NO-CO abatement are obtained with cobalt-aluminum mixed oxide catalyst. The impact of water was also investigated and following trends were obtained: (i) a decrease in activity for NO oxidation while no modification was observed for CO oxidation; (ii) a shift towards higher temperature for NO reduction while maintaining the same yield; (iii) an improved stability of the catalyst with time on stream.

Keywords: NO-CO reaction, Environmental Catalysis, Oxyfuel Combustion, Heterogeneous Catalysis, Transition Metal; Hydrotalcite

1. Introduction

CO_2 is the most produced greenhouse gas. Its emission in the atmosphere significantly contributes to the global warming. Consequently, scientific community focused on CO_2 capture/transformation, especially for application on large stationary sources such as electricity-generating power plants and Carbon Capture, Utilization, and Storage (CCUS) technologies become of prime importance in view of a control of CO_2 industrial emissions [1,2]. Complete or partial recycling of the CO_2 with a coupling reagent into high energy density liquids or fuels appears as an attractive strategy. Several other reactions such as artificial photosynthesis, photocatalysis, and heterogeneous catalysis to chemical and fuels, have been proposed as alternative for the CO_2 recycling. Nevertheless, all these applications need purified sources of CO_2 [3]. As potential CO_2 feed, is the Oxyfuel Combustion exhaust from large stationary sources like power plants or heavy industrial (cement or steel works...). Oxyfuel Combustion operates with fuel oxidation under nearly pure oxygen instead of air. Exhaust gas is composed of concentrated CO_2, residual O_2 and water, with some undesirable pollutants like NO and CO, that are shadowing the CO_2 valorization [4,5]. A solution to get rid of these pollutants could be to make them react together. NO reduction by CO and CO oxidation reaction are well described reactions, the reaction considered between NO and CO that occurs is $NO + CO = N_2 + CO_2$. This reaction has been widely studied for automobile depollution, by three-way catalysis (TWC) with Pt, Rh and Pd based catalytic formulations [6–11]. Noble metals based catalysts are particularly efficient for NO-CO reaction, even if some of them are particularly sensitive to water and oxygen as Rh which deactivates [12]. Whereas in the case of TWC the reaction takes place under stoichiometric conditions, the challenge here is to succeed in this reaction in an oxidizing medium as the flue gas to treat contains an excess of oxygen and CO_2.

Noble metal substitution with less expensive, more abundant, elements such as transition metals is particularly interesting for stationary source exhaust purification, especially if sensitivity to water and oxygen is limited. Activity of transition metal oxide for CO oxidation is particularly well documented [13], CuO and Co_3O_4 displaying activities comparable to noble metal formulations [14] and many researchers paid attention to the performance of these metals. Although the extraction of copper and cobalt from mines currently poses ethical and environmental problems as for many other metals including noble ones, it should be noted that 50% of the copper used in the European Union comes from recycling and that the recycling trend is on the rise thanks to the development of specialized channels.

Unfortunately, recycling plays a minor role in the cobalt market (less than 10% of total cobalt supply). However, many efforts are spent in this way, for example on lithium-ion batteries containing cobalt to recover valuable metals. In the long term, these recycling concepts are expected to make a significant contribution to cobalt supply that will allow the development of new technologies based on this metal as CO_2 purification. Cu-containing catalysts display interesting activity for NO-CO reaction with a stoichiometric ratio [15–18], and also for NO_x reduction by other reducers (propene [19], ammoniac [20], methanol [21], ethylene [22,23]) and NO decomposition [24]. Cu^+ species are considered as active sites for NO reduction. Cobalt oxides, being active for CO oxidation under mild conditions [13,25,26], also present NO_x reduction activity at high temperature, > 350°C [27,28]. Oliveira Correa et al. [29] measured a higher activity for CuAl-based mixed oxide with respect to the monometallic CuO, for NO-CO reaction, and Tang et al. [30] also reported good activity for NiO-CeO_2 mixed oxide. Therefore, formation of mixed oxide phase (such as hydrotalcite phase) leads to better performance than simple mixing of two oxides, as demonstrated for CuAl-mixed oxide [29]. This was confirmed by Tang et al. [30] over NiO-CeO_2 mixed oxide, the solid solution leading to improved inter-facial interactions between Ni and Ce ions, and consequently activity toward NO reduction (with NO/CO ratio= ½) [30]. Importance of metal oxide association is also visible on the water tolerance of catalyst. While single Cu or Ce catalysts strongly deactivated under H_2O-containing flow at moderate temperature, far better stability and improved activity are obtained with CuCe-containing formulation [31]. Cu^+ ions and oxygen vacancies formation in these binary oxides are suggested to be at the origin of the performance's enhancement. However, such improvements are not always observed, and Deng et al. [32] noticed for example drop in catalyst performance with CuO/CeO_2 and CuO/MnO_x-doped CeO_2 when 10 % of H_2O is added to the feed. Water affected both the reduction of NO and the selectivity towards N_2. Authors explained these results by the competition of NO and H_2O adsorption over Cu^+ sites.

Although the operating conditions are different, the aim of this study is to check if these materials can be nevertheless used for the NO+CO reaction. Thus, we are reporting the preparation of Co-Al and Cu-Al mixed oxides by using the hydrotalcite precursor (via Layer Double Hydroxide, LDH) for the NO-CO reaction in the presence of CO_2 and H_2O in the feed, under conditions of concentration and flow simulating exhaust from oxycombustion units. Comparison with monometallic copper and cobalt oxides allows determine the interest of using mixed phases as catalyst precursor.

2. Experimental

2.1. Catalysts preparation

Co or Cu-Al hydrotalcite like (HT) materials are synthesized by total substitution of Mg in $Mg_6Al_2(OH)_{16}CO_3.4H_2O$ LDH original material. The different samples were prepared by precipitation of metal nitrate salts: $Co(NO_3)_2$. $6H_2O$ (CHEMLAB, 97 wt.%), $Cu(NO_3)_2$. $3H_2O$ (PANREAC, 98.1 wt.%), $Al(NO_3)_3$. $9H_2O$ (Acros-Organics, 99 wt.%). The solution containing the metal precursors is added dropwise to 30 cm^3 of a solution of Na_2CO_3 (1M) (ACROS, 99.5 wt.%) under stirring while keeping the pH at a constant value of 10 by continuous adding of NaOH solution (2M) (PANREAC, 98 wt.%). Once the precursors solution is added, the mixture is stirred for 18 h at room temperature. The produced precipitate is then filtered and washed with deionized water at 60 °C. The solid is finally dried in an oven at 60 °C for 48 h. The dried materials were named as follows: Co_6Al_2-HT and Cu_6Al_2-HT.

Thereafter, the samples are calcined at 500 °C for 4 h under air flow of 60 mL/min (temperature increase rate of $1°C.min^{-1}$). The calcined materials are named as follows: Co_6Al_2 and Cu_6Al_2. In order to evaluate the effect of using HT phase as precursor to obtain Co_6Al_2 and Cu_6Al_2 oxides, Co_3O_4 and CuO are prepared by precipitation method.

2.2. Physico-chemical characterization

X-ray diffraction was performed using a Brücker D8 Advance diffractometer, equipped with a copper anticathode (λ = 1.5406 Å) and LynxEye type detector. Measurement program applied consists in: 2θ from 10° to 80°, step size = 0.02 °, integration time = 2 s per step. Crystalline phases were identified by comparison with the JCPDS database established by the ICDD.

Specific surface areas were determined applying the B.E.T. method (Brunauer, Emmet and Teller). Experiments were performed, after vacuum treatment at 100 °C for 2 h, on a Q Surf M1 system.

X-ray photoelectron spectroscopy (XPS) analyses were performed with a Kratos Axis Ultra, equipped with a dual Mg/Al anode and a monochromatized Al Kα source (1486.6 eV). The sample were analyzed as pellets, mounted on a double-sided adhesive tape. The pressure in the analysis chamber was in the range of 10^{-9} mbar during data registration. The binding energies were referred to the C1s component positioned at 284.8 eV. Atomic concentrations were calculated from peak intensity using the sensitivity factors provided with the Casa XPS

software (version 2.3.16 PR 1.6). The binding energy values are quoted with a precision of ±0.15 eV and the atomic percentage with a precision of ±10%.

Reducibility of materials was evaluated using H_2-temperature programmed reduction (H_2-TPR). Experiments were carried out using an Autochem II 2920 chemisorption analyzer equipped with a TCD detector (Micromeritics instrument). The samples (~20 mg) were loaded in a U-shaped quartz reactor and purged under N_2. Catalysts were then heated to 150 °C (10 °C.min^{-1}) during 1 h. This temperature ensures the water removal, as it was previously reported [33,34]. After cooling down to room temperature, a flow of 5 vol.% H_2 in Ar (30 mLmin^{-1}) passed through the catalyst and the reduction was performed by increasing the temperature up to 500 °C (5 °C.min^{-1}).

2.3. Catalytic tests

The catalysts (150 mg) were sieved between 0.315 and 0.500 mm, and diluted to a constant volume by SiC before being loaded in a quartz tubular reactor. The experiments were carried out at constant GHSV = 22 400 h^{-1}. Before reaction, the catalyst was pretreated under He flow (40 mL.min^{-1}) at 200 °C for 90 min for water removal. Then, the reactant flow was stabilized at total flow of 200 mL.min^{-1}. Flow is composed of 20 % CO_2, 10 % O_2, 0.5 % CO and 0.02 % NO (He as eluent gas) with or without 8.2 % of water. Reaction was conducted between 50 °C to 500 °C. The reaction products were analyzed by a gas chromatograph (Label GAS analyzer XXL1300), NO was analyzed with Xentra 4900C analyzer (Servomex). The measurement of NO_2 is performed indirectly using a NO_2 to NO converter BÜNOx (Bühler Technologies) by comparison. In order to evaluate the selectivity of the catalysts especially for N_2O, we used a room-temperature continuous-wave (CW) external cavity quantum laser cascade (EC-QCL) -based optical sensor described in a previous paper [35]. The conversion (X), selectivity (S) and yields (Y) are calculated according to the following equations:

$X_i\ (\%) = \frac{n_i^{int} - n_i^{out}}{n_i^{int}} * 100$ where n_i^{int} and n_i^{out} are number of moles of the corresponding compounds "i" (CO or NO) at the inlet and the outlet of the reactor.

$S_i\ (\%) = \frac{v_1 n_i}{\sum_{v_1} n_i} * 100$ or $\frac{n_i}{\sum_i n_i} * 100$ as $\nu_i = 1$

$Y_i(\%) = X_i * S_i * 100$

3. Results and discussion

3.1. Structural characterization

Figure **1** displays the XRD patterns obtained for the dried solids. Patterns evidence the formation of the hydrotalcite phase with visible reflections at 2θ = 11.3°; 22.8°; 34.5°; 38.6°; 45.5°; 60° and 62°, indexed to the lattice planes: (003), (006), (012), (015) (018), (110) and (113). The planes exposed are indicating the arrangement within Layer Double Hydroxide (LDH) network. In the case of Cu_6Al_2 sample, reflections associated to the formation of Malachite ($Cu_2(OH)_2CO_3$ sheet; PDF 01-075-1163) are also observed. The formation of malachite is associated to the low stability of Cu^{2+} ions in the LDH phase due to the Jahn-Teller effect [36,37].

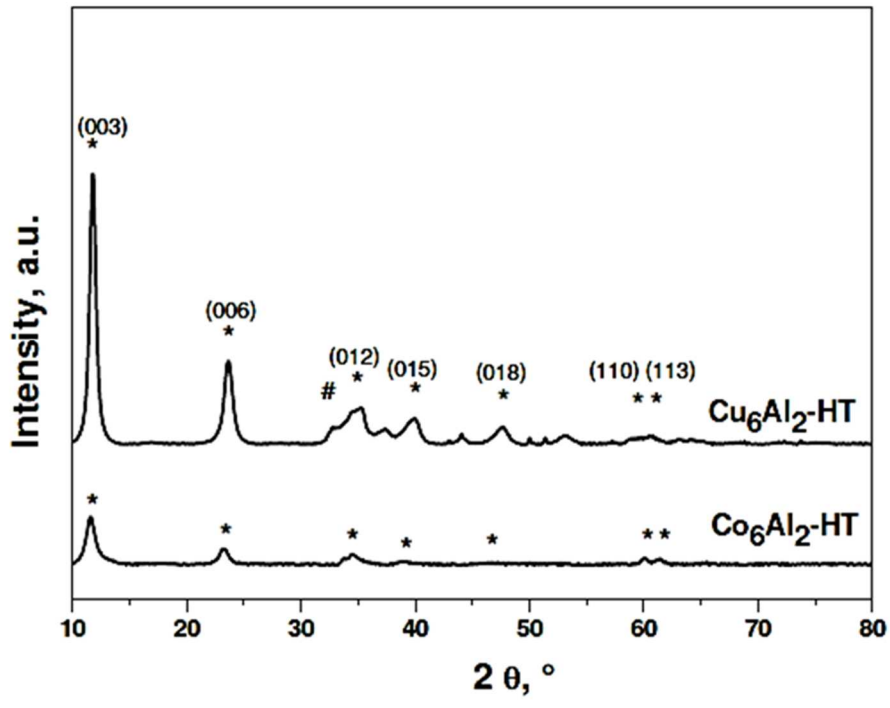

Figure 1. XRD patterns obtained for Cu_6Al_2-HT and Co_6Al_2-HT (dried sample); *: hydrotalcite PDF 22-0700; # : $Cu_2(OH)_2CO_3$ PDF 01-075-1163.

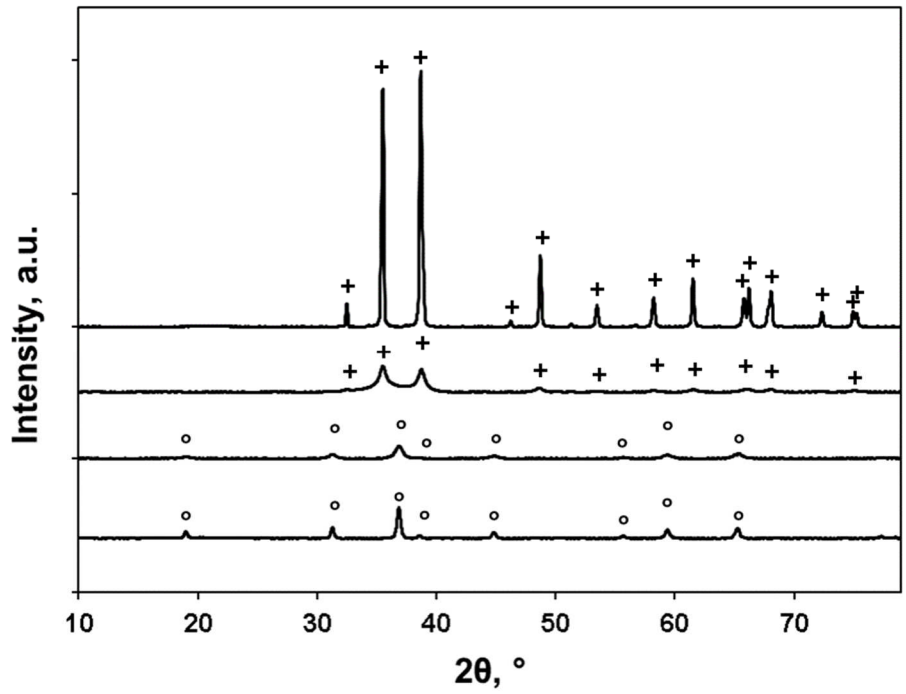

Figure 2. XRD patterns of calcined materials. +: CuO (PDF 48-1548); °: Co_2AlO_4 (PDF 38-0814) or $CoAl_2O_4$ (PDF 44-0160) or Co_3O_4 (PDF 42-1467).

The XRD patterns for calcined samples are shown in Figure **2**. The disappearance of the hydrotalcite phase and the formation of single and mixed-oxide phases upon calcination is confirmed as previously observed [38,39]. The diffractogram obtained for the Co_6Al_2 sample indicates the presence of cobalt or cobalt-aluminum spinel phases. Indeed, visible reflections and relative intensities fit with the Co_3O_4 (PDF 42-1467), Co_2AlO_4 (PDF 38-0814) and $CoAl_2O_4$ (PDF 44-0160) references. For the Cu_6Al_2 sample, only CuO phase is visible (PDF 48-1548). Indeed, the formation of copper spinel phase was observed only after thermal treatment at high temperature (> 700°C) [40,41].

The Co_3O_4 and CuO references display low specific surface areas (SSA) of 18 and 1 m^2g^{-1}, respectively. For the mixed-metal samples, SSA of the dried materials depends on the divalent cation (i.e. Cu or Co). The Co_6Al_2-HT sample shows the highest SSA (90 m^2 g^{-1}) while slightly lower SSA is reported for the Cu_6Al_2-HT sample (71 m^2g^{-1}). Calcination at 500 °C of hydrotalcite materials does not result in significant modifications of the SSA, which remains far above the values obtained for the single oxides. Indeed, SSA of 71 m^2 g^{-1} and 104 m^2 g^{-1} are obtained for Cu_6Al_2 and Co_6Al_2, respectively. Calcination step induces the removal of H_2O and CO_3^{2-} anions from the interlayers [23]. Hydrotalcite phase decomposition leads to a SSA increase in the case of Co-containing phase while the effect is negligible for Cu-

containing phase. The absence of notable effect on the SSA in the case of Cu_6Al_2 can be associated to the presence of not decomposed carbonate ions after treatment at 500 °C. Indeed, Chmielarz et al. [6] demonstrated that complete decomposition of copper-containing hydrotalcite phase occurs only at temperature above 550 °C.

3.2. Oxide reducibility

The evolution of the reducibility was investigated for Cu/Co calcined samples. The TPR profiles are exposed in Figure 3 and the reducibility properties are summarized in Table 1.

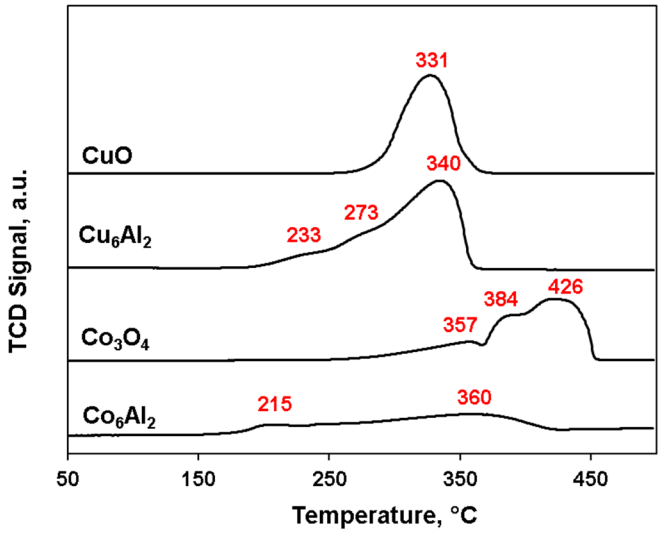

Figure 3. Temperature programmed reduction profile obtained for calcined samples.

Table 1. Reduction characteristics of calcined samples.

Sample	Reduction temperature, °C	H_2 consumed, mmol g^{-1}	Reduction degree, %
CuO	331	14.3	88
Cu_6Al_2	233; 273; 340	10.6	72
Co_3O_4	357; 384; 426	15.6	94
Co_6Al_2	215, 360	4.2	43

Reduction profile obtained for Co_3O_4 occurs in two main steps, as classically observed [22], with the successive reduction of Co(III) into (Co(II) and of Co(II) into Co(0) as depicted in the two following equations:

$$Co_3O_4 + H_2 = 3\ CoO + H_2O$$

$$CoO + H_2 = Co^0 + H_2O$$

Reduction mostly occurs above 350 °C, and the amount of H_2 allows to determine a reduction degree of Co(III) to Co(0) of 94% at the end of the experiment (Table 1). Temperatures of reduction for the two successive steps, at 384 °C and 426 °C, are close to the values reported for the reduction of cobalt spinel [42]. In the case of the Co_6Al_2 sample, reduction starts at lower temperature, i.e. at ~180 °C, with a main consumption located at 360 °C. However, the total amount of H_2 consumed is divided by 3.7 when compared with the value obtained for Co_3O_4. The total amount of H_2 consumed leads to a reduction degree of cobalt (assuming Co(II) at initial state) to Co(0) of 43% (Table 1) that is far below the value obtained for Co_3O_4. These results demonstrated the stability of the ionic cobalt when inserted in the hydrotalcite phase since at the end of the experiment, the reduction is not achieved. The broad, low temperature, reduction peak observed between 180 °C and 360 °C can be associated to the presence of small CoOx oxide particle reduction located at the surface of the material.

The reduction profile obtained for the CuO sample displays only one main hydrogen consumption. According to the literature, the reduction of Cu(II) from CuO to Cu(0) occurs in one step. The value of H_2 consumed, 14.3 mmol g^{-1} (Table 1) confirms the single step reduction to metal copper since a reduction degree of 88% is calculated, which can be considered as an almost complete reduction. The temperature at which the reduction occurs, i.e. 300-350°C, refers to the reduction of large CuO crystals [43]. The reduction profile obtained for Cu_6Al_2 slightly differs since the reduction starts at lower temperature, ~200°C. This first reduction can be associated to the reduction of highly dispersed CuO species [44]. The second hydrogen consumption, located at 233 °C, is related to the reduction of Cu(II) from the $CuAl_2O_4$ spinel to Cu(0) [45,46]. Previous results show that spinel prepared by solid phase method exhibits a multi peak distribution. The first, denoted as (α) and located at lower temperature, is attributed to the reduction of highly dispersed copper oxide species. The peak denoted as (β) is attributed to peak β to spinel-type Cu species. The peak located at higher temperature (γ) is assigned to hardly-reducible spinel-type Cu species [47,48]. From the quantity of hydrogen consumed, a reduction degree of Cu(II) to Cu(0) of 72% is calculated, showing that most of the copper, even when located in the spinel phase, is reducible at low to intermediate temperature.

3.3. Surface characteristics

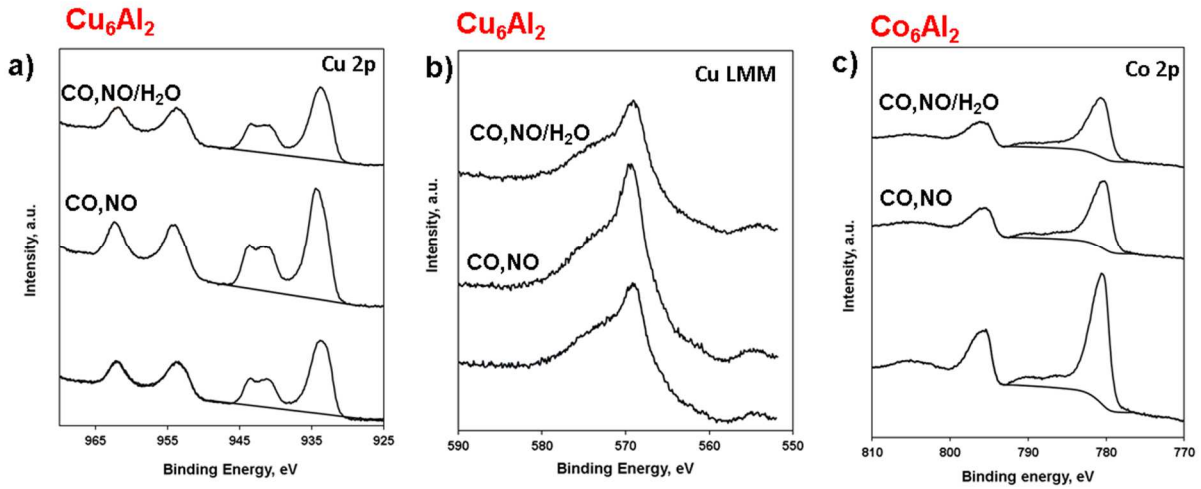

Figure 4. Core level spectra of: (a) Cu 2p and (b) Cu LMM obtained for Cu_6Al_2; (c) Co 2p obtained for Co_6Al_2 (calcined forms).

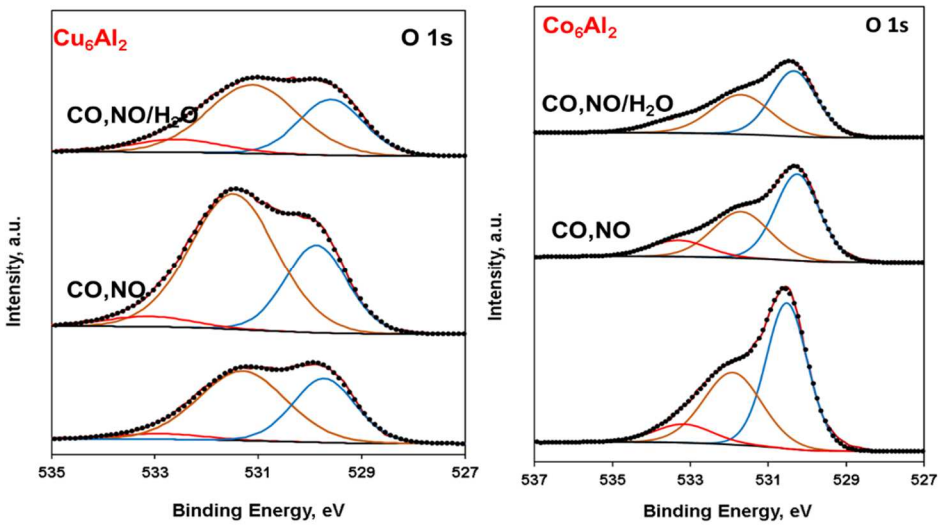

Figure 5. O 1s core level spectra of (a) Cu_6Al_2 and (b) Co_6Al_2 (calcined forms).

XPS analysis was performed for Cu_6Al_2 and Co_6Al_2 materials. The spectral parameters are summarized in Table 2 and the respective surface composition is listed in Table 3.

The Cu 2p spectrum obtained for the calcined Cu_6Al_2 sample is presented in Figure 4(a). The spectrum displays a main contribution for Cu 2p3/2 of 933.4 to 933.8 eV and 2p1/2 of 953.4 to 953.8 eV (Table 2) for the fresh and spent catalysts respectively, this B.E. is corresponding to the presence of Cu(II) species from CuO phase or from the mixed oxide phases. Moreover, the confirmation of the CuO phases (Cu(II) species) is revealed by the visible shake-up satellite, exposed for all copper containing materials. Cu species LMM Auger was also investigated and the spectra are presented in Figure 4(b); the Auger parameter was determined and is listed in Table 2 [49]. Both the Cu LMM Auger KE of 917.3-917.7 eV and the Auger

parameter of 1851.2-1851.9 are confirming the Cu^{2+} species presence for the mixed oxide material and also for the catalyst recovered after the test with NO/CO and NO/CO-H_2O) [50].The spectrum obtained for the Co 2p core level for Co_6Al_2 sample is presented in Figure 4(c). The spectrum presents the main contributions for Co 2p3/2 at 780.0-780.2 eV and Co 2p1/2 at 795.5-756.0 eV, thus confirming the presence of both Co(II) and Co(III) within Co_3O_4 spinel phase [49]. The distance of the two spin-orbit doublets was calculated, as is giving information regarding the presence of the Co_3O_4 phases. A value of 15.3- to 16.0 eV is measured, consequently, the presence Co_3O_4 spinel phase is confirmed [50]. Al 2p spectra, with a contribution at 73.5 to 73.9 eV (Figure 5), is revealing the formation of Al^{3+} species from the Al_2O_3 phases for the Cu and Co based materials [50]. From a surface composition point of view, the Al/M (M = Cu or Co) ratios obtained for the calcined samples (Table 3) show values of 0.40 (Cu_6Al_2) and 0.36 (Co_6Al_2) that are little above the theoretical bulk composition which should lead to a ratio of 0.33, this may be due to incomplete incorporation of the transition metal within the hydrotalcite layer over the synthesis. Finally, the O 1s spectra are presented in Figure 6. Three components are distinguished: (i) the contribution located at BE = 529.1-530.5 eV is ascribed to surface lattice oxygen (O^{2-}), denoted O_{latt}; (ii) the contribution at BE = 531.1 eV-531.9 eV is associated to adsorbed oxygen species (O^2(ads) and O^-), denoted O_{ads}; (iii) the last contribution at the highest BE (533.3 eV) is associated to the oxygen species in adsorbed water or hydroxyl groups. The O_{ads}/ O_{latt} was calculated using the area of the decomposed curves (Table 2) [45,50]. O_{ads}/O_{latt} ratios of 1.51 and 0.59 are calculated for Cu_6A_{l2} and Co_6Al_2 respectively. An enrichement in oxygen adsorbed species on the surface of the copper containing material is then clearly observed (Table 2).

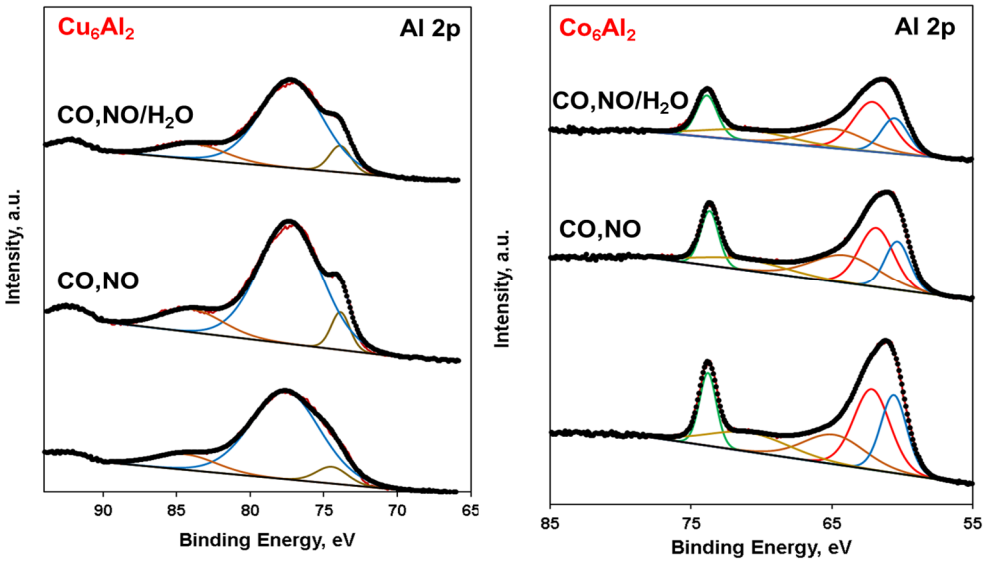

Figure 6. Al 2p core level spectra of (a) Cu_6Al_2 and (b) Co_6Al_2 (calcined forms)

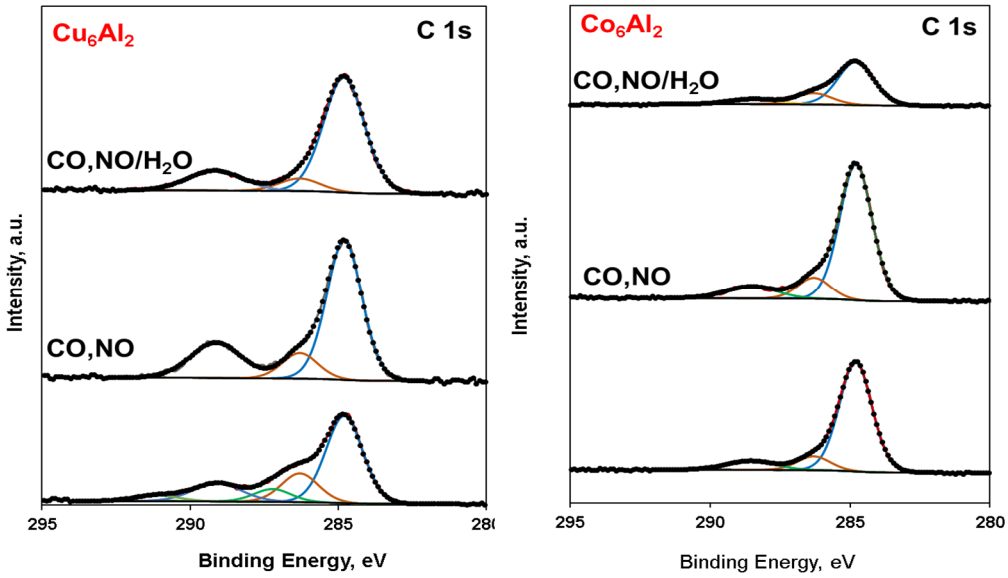

Figure 7. C 1s core level spectra of (a) Cu_6Al_2 and (b) Co_6Al_2 (calcined forms)

The C 1s spectra are ilustrated in Figure 7. The spectra recorded for all samples are composed of three components located at 284.8 eV, 286.3 eV and 289.1 which are assigned to adventitious carbon (C-C, C-O-C, and O-C=O groups) [49]. Analysing the carbon at% for the spent catalyst in the case of Co_6Al_2, after CO,NO test we observed an enrichment with carbon with 37% higher than for the fresh material (Table 3).

Table 2. Spectral parameters obtained for Cu_6Al_2 and Co_6Al_2.

Sample	Treatment	Cu $2p_{3/2}$ eV	Cu LMM[a] eV	α^b eV	Co $2p_{3/2}$ eV	Co $2p_{1/2}$ eV	ΔCo 2p eV[c]	Al 2p, eV	O 1s eV	O_{ads}/O_{latt} [d]
Cu_6Al_2	calcined	933.8	917.7	1851.5	-	-	-	73.8	529.7 (37.9) 531.3 (57.4) 532.9 (4.64)	1.51
	CO,NO	933.9	917,3	1851.2	-	-	-	73,8	529.1 (30.11) 531.4 (64.95) 533.1 (4.95)	2.10
	CO,NO/ H_2O	933.4	917.7	1850.9	-	-	-	73,7	529.5 (32.83) 531.1 (56.52) 532 (10.65)	1.72
Co_6Al_2	calcined	-	-		780.2	795.5	15.3	73.8	530.5 (53.42) 531.9	0.69

									(37.07) 533.1 (9.51)	
	CO,NO	-	-		780.0	796.0	16	73.7	530.2 (51.27) 531.7 (35.88) 533.3 (2.85)	0.69
	CO,NO/ H_2O	-	-		780.2	795.9	15.7	73.9	530.3 (49.04) 531.7 (38.7) 533.3 (12.26)	0.78
								73.6		
								73.5		
								73.5		

[a], Cu Auger (LMM); [b], α is the Auger parameter Cu $2p_{3/2}$ BE (eV) + Cu Auger, KE (eV); [c], ΔCo2p = Co $2p_{1/2}$ - Co $2p_{3/2}$ (eV); [d], ratio between the O_{latt} (contribution at 529.7-530.3 eV) and O_{ads} (contribution at 531.3-531.9 eV) species.

Table 3. XPS-calculated surface composition obtained for Cu_6Al_2 and Co_6Al_2.

Sample	Treatment	Cu/ at.%	Co/ at.%	Al/ at.%	Al/M	O/ at.%	C/ at.%
Cu_6Al_2	Calcined	17.1	/	6.8	0.40	47.2	28.9
	CO,NO	17.0	/	5.4	0.32	52.7	25.0
	CO,NO/H_2O	15.9	/	7.2	0.46	46.8	30.1
Co_6Al_2	calcined	/	21.0	7.6	0.36	46.4	25.1
	CO,NO	/	14.6	7.6	0.52	37.7	40.1
	CO,NO/H_2O	/	20.5	10.0	0.49	46.5	23.1

3.4. Catalytic properties of oxide

Water free conditions

Light-off conversion curves obtained for the different samples are shown in Figure 8. For all the oxides, and under the conditions of reaction selected, CO is completely oxidized into CO_2 below 275 °C. Temperatures for 50 % and 90 % conversions are listed in Table 4.

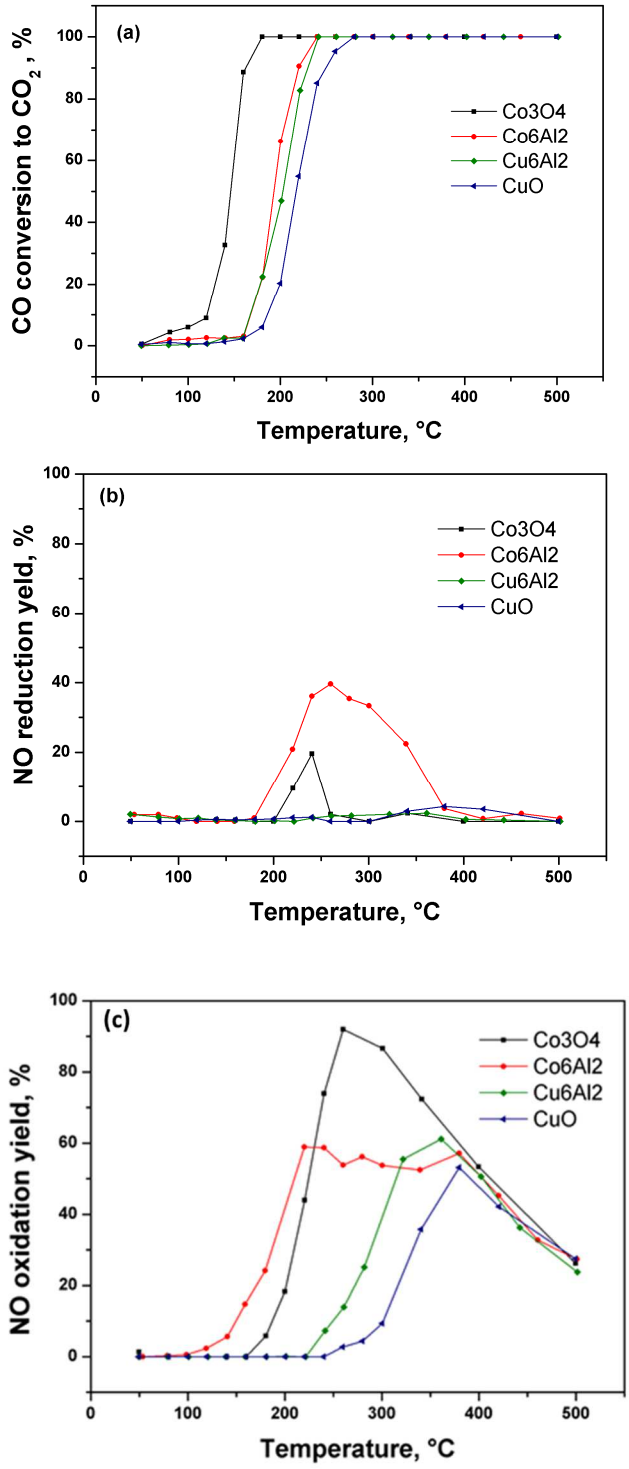

Figure 8. Catalytic results obtained for the different calcined oxide catalysts: (a) CO oxidation to CO_2; (b) NO reduction yield; (c) NO oxidation yield. Reaction performed without water added to the feed.

Pure cobalt oxide, Co_3O_4, presents the best activity, with the lowest T50 and T90 temperatures. Co_6Al_2 and Cu_6Al_2 are presenting comparable performances in CO oxidation,

with T50 and T90 approximatively 40 °C above those of Co_3O_4. Finally, CuO presents the lowest activity with T50 and T90 approximatively 60 °C above those of the Co_3O_4. The results obtained are in adequacy with references where it was described that some cobalt oxides are excellent catalysts for the CO oxidation, even if remaining less active than supported noble metals [13,25,26]. The origin of the activity of cobalt oxides is associated to the cobalt reducibility, Co^{3+}/Co^{2+}, and to CO adsorption properties [51]. From a mechanism point of view, CO is expected to adsorb onto low oxidation state Co atoms (Co^{2+} species) [52]. CO(ads) thereafter reacts with active surface oxygen bonded to Co^{3+} species to form CO_2. Reaction is resulting in formation of oxygen vacancies and reduction of cobalt site. Reduced cobalt reoxidizes by dissociative adsorption of O_2(g) [52]. The slightly lowest activity measured for Co_6Al_2 could be explained by the reducibility properties of these materials. Indeed, the Co_6Al_2 sample starts to reduce at lower temperature than Co_3O_4. However, the total amount of reducible/reoxidizable Co sites is significantly lower (3.7 times lower hydrogen consumption below 450 °C for the Co_6Al_2 than for the Co_3O_4 sample) despite the highest surface area displayed by the Co_6Al_2, sites suggested to be active for the CO oxidation.

The Cu_6Al_2 catalyst is presenting comparable activity than the Co_6Al_2 catalyst. The catalytic properties could be related to the ease of Cu^{2+} to reduce in Cu_6Al_2 catalyst which exhibits sufficient surface area to expose reducible copper surface sites. On the contrary, the CuO sample, which also presents reducibility at low temperature, is displaying the lowest catalytic activity. However, the very limited surface area obtained for this material, 1 m^2g^{-1}, is clearly at the origin of the low activity obtained.

Table 4. Temperature for 50% conversion (T50) and 90% conversion (T90) CO conversion on the different samples (calcined form).

Catalysts	T_{50} (°C)	T_{90} (°C)
CuO	217	250
Cu_6Al_2	204	228
Co_3O_4	148	163
Co_6Al_2	193	220

NO reduction curves show that only Co-containing catalysts are able to reduce NO, and that the reduction reaction starts at a temperature comparable to the temperature at which CO starts to be converted (175-200 °C) (Figure 6(b)). At around 340 °C, a drop in NO conversion was observed due to the consumption of the CO by the oxidation reaction, and to the increase in NO stability at higher temperatures [53]. Far better reduction performance is obtained with the Co_6Al_2 catalyst, with 20 % NO reduction between 220 °C and 340 °C, and 40 % reached at 260 °C. On the contrary, no NO reduction activity is observed, under the conditions of reaction applied (CO_2 and O_2 present in the reaction feed), with the Cu_6Al_2 and CuO catalyst. No formation of N_2O was observed. The poor activity obtained by the CuO and Cu_6Al_2 catalysts could be associated to the high oxygen concentration in the reaction feed (10 vol.%). Iwamoto et al. [54] reported a complete loss of NO decomposition activity over copper catalyst (3.6 % Cu-ZSM-5) in presence of 10 % O_2 at comparable temperature than used for this study. Chmielarz et al. [20] however showed that copper catalysts issued from hydrotalcite phases are more efficient for NO reduction than Cu- and Co-oxides, which is the opposite of what we observed. This difference in reactivity could however originate from the reducer used (NH_3) and obviously to the lower O_2 concentration applied in this study (2.5 vol.%).

Finally, under the conditions of reaction applied, NO conversion leads to the production of NO_2 for all catalysts. Cobalt containing catalysts are the most active, while significantly lower activity is obtained with copper catalysts (Figure 6(c)). On the contrary to what was observed for the CO oxidation, the best activity is measured for the Co_6Al_2 catalyst, which is more active than Co_3O_4. A significantly shift of the NO oxidation curves are observed for the two Cu catalysts, the CuO materials being again the less active probably due to its inadequate textural properties. The formation of NO_2 is obviously associated to the presence of 10 vol.% O_2 in the reaction feed. According to thermodynamic data, excess of O_2 is in favor of all nitrogen oxides concentration [55] due to the inhibition of NO decomposition reaction, and the displacement of the oxidation reaction equilibrium in favor of the oxidized compounds.

The reaction has limited effect on the surface characteristics of materials, as analyzed by XPS. In the case of Co_6Al_2, the Co 2p and O 1s core level spectra are poorly affected by the reaction. The ΔCo 2p value slightly increases from 15.3 eV (fresh sample) to 16.0 (after CO-NO reaction under water free condition) (Table 2) which does not denote of a significant change in Co^{3+}/Co^{2+} environment that remains of spinel type. The Al/Co atomic ratio also slightly increases, from 0.36 (fresh catalyst) to 0.52 (after reaction). Finally, the O_{ads}/O_{latt}

which can be considered as a indication of the reactive surface oxygen species, is not affected by the reaction (constant value of 0.69 obtained before and after reaction). As the Cu^+ species are considered to be active toward the NO reduction, we investigate for Cu_6Al_2 catalyst, the formation of Cu^+ for the samples recovered after catalytic test. The Auger parameter for the fresh sample is of 1851.5, after catalytic test Auger parameter is of 1851.2 eV for water free reaction and 1850.9 eV respectively for water reaction, corresponding to the presence of Cu^{2+} species. The Al/Cu ratio is slightly modified in favor of the Cu abundance on the surface (0.40 before reaction vs. 0.32 after reaction), which fits with the O_{ads}/O_{latt} ratio evolution (1.51 before reaction; 2.10 after reaction) considering that the oxygen reactive species will preferably locate on reducible copper sites.

Performances in presence of water

The water effect on CO oxidation and NO reduction in an oxidizing medium was also studied on the Co_6Al_2 which showed highest conversion for both reactions. For the reaction, 8.2 vol.% H_2O is added to the reaction flow composed of 20 vol.% CO_2 - 10 vol.% O_2 - 0.5 vol.% CO -0.02 vol.% NO and the light -off curves are presented in Figure 9. The results show that presence of water has no influence on the Co_6Al_2 catalyst performance for the CO oxidation reaction, the light-off curves being located at comparable temperatures. Then the catalyst is particularly tolerant to water presence. The presence of water however significantly impacts NO oxidation and NO reduction yields. For NO reduction, Co_6Al_2 kept its maximum activity at ~40% (as in the case of reaction under water free conditions). However, the yield curve shifts by 60 °C towards higher temperatures. No formation of N_2O was observed. A strong promoting effect of the water presence is observed on the NO oxidation yield curve which is shifted by 80 °C toward the lower temperatures. In addition, the NO oxidation yield is significantly dropped, leading to a yield divided by two.

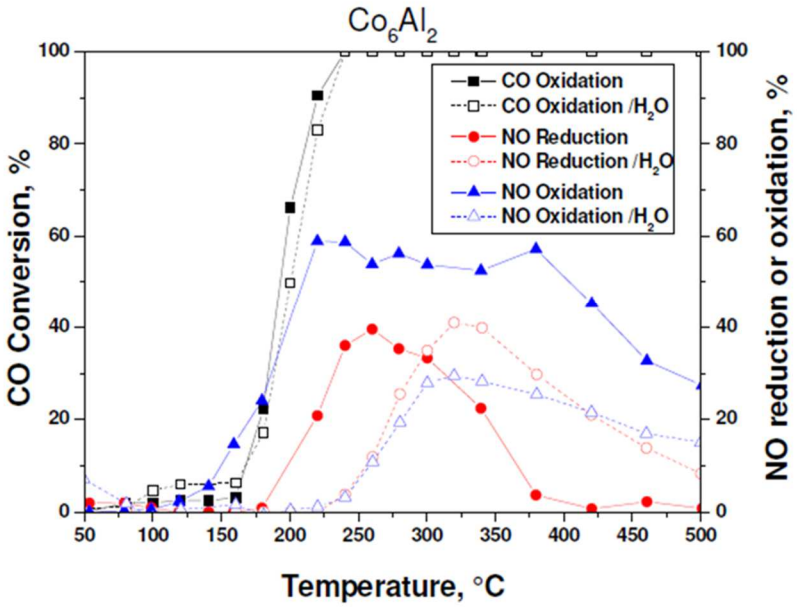

Figure 9. Evolution of CO conversion and NO reduction and oxidation yields as a function of temperature with Co_6Al_2 in the absence and presence of 8.2 % H_2O added to the feed.

After reaction in presence of water, the Co_6Al_2 surface catalyst is not profoundly modified. The ΔCo 2p is close to that obtained after reaction under water free conditions meaning that the cobalt average valence remains constant. The Al/Co ratio is remaining around 0.5. Only the O_{ads}/O_{latt} is observed to slightly increase which is coherent with catalytic results considering that the oxidation activity is, even if not promoted for CO oxidation reaction, improved in the case of NO oxidation. This increase in oxygen adsorbed on the surface of the catalyst may also explain why we have a change in the selectivity of the products and in particular a decrease in the formation of NO_2. Indeed, Chinchen et al. have shown that the presence of oxygen on the surface of their copper-based catalyst facilitates the water-gas shift reaction [56]. This was also demonstrated more recently in a DFT study by Tang et al [57]. Thus, favoring the water-shift reaction makes it possible to produce hydrogen, a more powerful reducing agent than CO, thus reducing the formation of NO_2.

4. Conclusion

We are reporting the preparation of copper and cobalt mixed oxides derived from hydrotalcite. CuO and Co_3O_4 were used as reference. All the materials were characterized after drying, for analyzing the hydrotalcite phases and after calcination for analyzing the oxide phases by XRD, N_2-physisorption, H_2-TPR and XPS. The XRD are confirming the formation of the hydrotalcite crystalline phases. The preparation route is evidencing higher

SSA for hydrotalcite and mixed oxides that the Cu and Co bulk references. The hydrotalcites derived Cu and Co are exposing lower reduction temperature than the bulk counterparts (215 °C and 357 °C for Co_6Al_2 and 230 °C to 340 °C for Cu_6Al_2).

The catalytic performance of cobalt and copper mixed oxides for CO_2 purification derived from oxycombustion in absence or presence of water were investigated. Preparation of mixed oxide by the hydrotalcite way led to an improvement of CO oxidation and NO reduction. The same activity trend was obtained for the two reactions studied (simultaneous CO oxidation and NO reduction): CuO < CuAl < CoAl<Co_3O_4. The most efficient catalyst Co_6Al_2 exhibited the most important NO reduction (40 % at 260 °C) with total CO oxidation at low temperature (around 250 °C).

We also investigated the impact of the presence of 8.2 % water in the reaction stream on the catalytic activity, the catalyst of Co_6Al_2 was selected, as it was showing the highest performances into the reactions studied. It appeared that the presence of water had a different effect on the different reactions. The CO oxidation is not affected, the NO reduction yield is unchanged but delayed and the NO oxidation is decreased. So, water has a beneficial effect on the reaction. This is due to the reaction ($CO+H_2O = CO_2+H_2$) called WGS also influenced the NO reduction.

Acknowledgements

The authors thank the Greater Dunkirk Council (CUD), Dunkerque LNG, Innocold and ULCO university for the financial support. The authors thank the Chevreul Institute (FR 2638) for its help in the development of this work. Chevreul Institute is supported by the « Ministère de l'Enseignement Supérieur et de la Recherche et de l'Innovation », the « CNRS » the « Région Hauts-de-France », the « Métropole Européenne de Lille » and the « Fonds Européen de Développement des Régions. Pardis Simon is acknowledged for XPS analysis.

References

[1] M. Pérez-fortes, J.A. Moya, K. Vatopoulos, E. Tzimas, CO 2 Capture and Utilization in Cement and Iron and Steel Industries, Energy Procedia. 63 (2014) 6534–6543. https://doi.org/10.1016/j.egypro.2014.11.689.

[2] R. Stanger, T. Wall, R. Spörl, M. Paneru, S. Grathwohl, M. Weidmann, G. Scheffknecht, D. Mcdonald, K. Myöhänen, J. Ritvanen, S. Rahiala, T. Hyppänen, J. Mletzko, A. Kather, S. Santos, International Journal of Greenhouse Gas Control Oxyfuel combustion for CO 2 capture in power plants, Int. J. Greenh. Gas Control. 40 (2015) 55–125. https://doi.org/10.1016/j.ijggc.2015.06.010.

[3] K.M.K. Yu, I. Curcic, J. Gabriel, S.C.E. Tsang, Recent advances in CO2 capture and utilization., ChemSusChem. 1 (2008) 893–899. https://doi.org/10.1002/cssc.200800169.

[4] K. Andersson, F. Normann, F. Johnsson, B. Leckner, NO emission during oxy-fuel combustion of lignite, Ind. Eng. Chem. Res. 47 (2008) 1835–1845. https://doi.org/10.1021/ie0711832.

[5] C. Iloeje, R. Field, A.F. Ghoniem, Modeling and parametric analysis of nitrogen and sulfur oxide removal from oxy-combustion flue gas using a single column absorber, Fuel. 160 (2015) 178–188. https://doi.org/10.1016/j.fuel.2015.07.057.

[6] P. Granger, V.I. Parvulescu, Catalytic NOx abatement systems for mobile sources: From three-way to lean burn after-treatment technologies, Chem. Rev. 111 (2011) 3155–3207. https://doi.org/10.1021/cr100168g.

[7] H. Permana, K.Y. Simon Ng, C.H.F. Peden, S.J. Schmieg, D.K. Lambert, D.N. Belton, Adsorbed Species and Reaction Rates for NO–CO over Rh(111), J. Catal. 164 (1996) 194–206. https://doi.org/http://dx.doi.org/10.1006/jcat.1996.0375.

[8] J. Barbier, D. Duprez, Steam Effects in 3-Way Catalysis, Appl. Catal. B-Environmental. 4 (1994) 105–140.

[9] W. Chen, Q. Shen, R. a Bartynski, P. Kaghazchi, T. Jacob, Reduction of NO by CO on unsupported Ir: bridging the materials gap., Chemphyschem. 11 (2010) 2515–20. https://doi.org/10.1002/cphc.201000254.

[10] A.A. Vedyagin, A.M. Volodin, V.O. Stoyanovskii, R.M. Kenzhin, E.M. Slavinskaya, I. V. Mishakov, P.E. Plyusnin, Y. V. Shubin, Stabilization of active sites in alloyed Pd-Rh catalysts on gamma-Al2O3 support, Catal. Today. 238 (2014) 80–86. https://doi.org/10.1016/j.cattod.2014.02.056.

[11] T. Maunula, J. Ahola, T. Salmi, H. Haario, M. Härkönen, M. Luoma, V.J. Pohjola, Investigation of CO oxidation and NO reduction on three-way monolith catalysts with transient response techniques, Appl. Catal. B Environ. 12 (1997) 287–308. https://doi.org/10.1016/S0926-3373(96)00084-7.

[12] D. Panayotov, M. Khristova, M. Velikova, Interactions NO-CO and O2-NO-CO on and on y-Al2O3- and CuCo2O4/ y-Al2O3-supported Pt , Rh and Pt-Rh catalysts , a transient response study, Appl. Catal. B Environ. 9 (1996) 107–132.

[13] S. Royer, D. Duprez, Catalytic Oxidation of Carbon Monoxide over Transition Metal Oxides, ChemCatChem. 3 (2011) 24–65. https://doi.org/10.1002/cctc.201000378.

[14] J.T. Kummer, Catalysts for automobile emission control, 5 (1982).

[15] V. Muñoz, F.M.Z. Zotin, L.A. Palacio, Copper–aluminum hydrotalcite type precursors for NOx abatement, Catal. Today. 250 (2015) 173–179. https://doi.org/10.1016/j.cattod.2014.06.004.

[16] F. Amano, S. Suzuki, T. Yamamoto, T. Tanaka, One-electron reducibility of isolated copper oxide on alumina for selective NO-CO reaction, Appl. Catal. B Environ. 64 (2006) 282–289. https://doi.org/10.1016/j.apcatb.2005.12.011.

[17] C.A. Sierra-Pereira, E.A. Urquieta-González, Reduction of NO with CO on CuO or Fe2O3 catalysts supported on TiO2 in the presence of O2, SO2 and water steam, Fuel. 118 (2014) 137–147. https://doi.org/10.1016/j.fuel.2013.10.054.

[18] X. Jiang, F. Du, X. Zhang, Y. Jia, X. Zheng, Catalytic properties of CuO/Sn0.9Ti0.1O2 and CuO/Sn0.7Ti0.3O2 in NO+CO reaction, J. Zhejiang Univ. A. 8 (2007) 1839–1845. https://doi.org/10.1631/jzus.2007.A1839.

[19] C. Marquez-Alvarez, I. Rodriguez-Ramos, A. Guerrero-Ruiz, G.L. Haller, M. Fernandez-Garcia, Selective reduction of NOx with propene under oxidative conditions: nature of the active sites on copper based catalysts, J. Am. Chem. Soc. 119

(1997) 2905–2914. https://doi.org/10.1021/ja961629y.

[20] L. Chmielarz, P. Kuśtrowskiai, A. Rafalska-Łasocha, D. Majda, R. Dziembaj, Catalytic activity of Co-Mg-Al, Cu-Mg-Al and Cu-Co-Mg-Al mixed oxides derived from hydrotalcites in SCR of NO with ammonia, Appl. Catal. B Environ. 35 (2002) 195–210. https://doi.org/10.1016/S0926-3373(01)00254-5.

[21] J.R.H. Ross, P. Clancy, The use of copper catalysts for the selective reduction of NO with methanol, Catal. Today. 137 (2008) 146–156. https://doi.org/10.1016/j.cattod.2007.10.115.

[22] S. Bennici, P. Carniti, A. Gervasini, Bulk and surface properties of dispersed CuO phases in relation with activity of NOx reduction, Catal. Letters. 98 (2004) 187–194. https://doi.org/10.1007/s10562-004-8679-9.

[23] S. Bennici, A. Gervasini, Catalytic activity of dispersed CuO phases towards nitrogen oxides (N2O, NO, and NO2), Appl. Catal. B Environ. 62 (2006) 336–344. https://doi.org/10.1016/j.apcatb.2005.09.001.

[24] T. Ohnishi, K. Kawakami, M. Nishioka, M. Ogura, Direct decomposition of NO on metal-loaded zeolites with coexistence of oxygen and water vapor under unsteady-state conditions by NO concentration and microwave rapid heating, Catal. Today. 281 (2017) 566–574. https://doi.org/10.1016/j.cattod.2016.07.012.

[25] X. Xie, Y. Li, Z.-Q. Liu, M. Haruta, W. Shen, Low-temperature oxidation of CO catalysed by Co3O4 nanorods., Nature. 458 (2009) 746–749. https://doi.org/10.1038/nature07877.

[26] a. Alvarez, S. Ivanova, M. a. Centeno, J. a. Odriozola, Sub-ambient CO oxidation over mesoporous Co 3O 4: Effect of morphology on its reduction behavior and catalytic performance, Appl. Catal. A Gen. 431–432 (2012) 9–17. https://doi.org/10.1016/j.apcata.2012.04.006.

[27] S. Zhuang, M. Yamazaki, K. Omata, Y. Takahashi, M. Yamada, Catalytic conversion of CO , NO and SO2 on supported sulfide catalysts II . Catalytic reduction of NO and SO2 by CO, 31 (2001) 133–143.

[28] G.L. Bauerle, N.T. Thomas, K. Nobe, Tungsten bronzes and mixed cobalt oxides as

potential catalysts for pollution control, Chem. Eng. J. 4 (1972) 199–200. https://doi.org/10.1016/0300-9467(72)80013-3.

[29] C.L. Oliveira Corrêa, Y.E. Licea, L. Amparo Palacio, F.M. Zanon Zotin, Effect of composition and thermal treatment in catalysts derived from Cu-Al hydrotalcites-like compounds in the NO reduction by CO, Catal. Today. 289 (2017) 133–142. https://doi.org/10.1016/j.cattod.2016.08.023.

[30] C. Tang, B. Sun, J. Sun, X. Hong, Y. Deng, F. Gao, L. Dong, Solid state preparation of NiO-CeO2 catalyst for NO reduction, Catal. Today. 281 (2017) 575–582. https://doi.org/10.1016/j.cattod.2016.05.026.

[31] B. Wen, M. He, Study of the Cu-Ce synergism for NO reduction with CO in the presence of O2, H2O and SO2 in FCC operation, Appl. Catal. B Environ. 37 (2002) 75–82. https://doi.org/10.1016/S0926-3373(01)00316-2.

[32] C. Deng, Q. Huang, X. Zhu, Q. Hu, W. Su, J. Qian, L. Dong, B. Li, M. Fan, C. Liang, The influence of Mn-doped CeO2 on the activity of CuO/CeO2 in CO oxidation and NO+CO model reaction, 389 (2016) 1033–1049. https://doi.org/10.1016/j.apsusc.2016.08.035.

[33] H. Dib, R. El Khawaja, G. Rochard, C. Poupin, S. Siffert, R. Cousin, CuAlCe Oxides Issued from Layered Double Hydroxide Precursors for Ethanol and Toluene Total Oxidation, Catal. . 10 (2020). https://doi.org/10.3390/catal10080870.

[34] A. Alejandre, F. Medina, X. Rodriguez, P. Salagre, J.E. Sueiras, Preparation and activity of copper, nickel and copper-nickel-al mixed oxides via hydrotalcite-like precursors for the oxidation of phenol aqueous solutions, Stud. Surf. Sci. Catal. 130 B (2000) 1763–1768. https://doi.org/10.1016/s0167-2991(00)80456-5.

[35] F. Shen, J. Akil, G. Wang, C. Poupin, R. Cousin, S. Siffert, E. Fertein, T.-N. Ba, W. Chen, Real-time monitoring of N2O production in a catalytic reaction process using mid-infrared quantum cascade laser, J. Quant. Spectrosc. Radiat. Transf. 221 (2018) 1–7. https://doi.org/10.1016/J.JQSRT.2018.09.022.

[36] A. Alejandre, F. Medina, P. Salagre, X. Correig, J.E. Sueiras, Preparation and Study of Cu-Al Mixed Oxides via Hydrotalcite-like Precursors, Chem. Mater. (1999) 939–948.

[37] R. Manivannan, A. Pandurangan, Formation of ethyl benzene and styrene by side chain methylation of toluene over calcined LDHs, Appl. Clay Sci. 44 (2009) 137–143. https://doi.org/10.1016/j.clay.2008.12.017.

[38] E. Genty, R. Cousin, S. Capelle, C. Gennequin, S. Siffert, Catalytic Oxidation of Toluene and CO over Nanocatalysts Derived from Hydrotalcite-Like Compounds ($X_6^{2+}Al_2^{3+}$): Effect of the Bivalent Cation, Eur. J. Inorg. Chem. (2012) 2802-2811 https://doi.org/10.1002/ejic.201101236.

[39] D. Hammoud, C. Gennequin, A. Aboukais, Production of hydrogen by steam reforming of methanol in the presence of copper / zinc-aluminium based catalysts prepared by adopting memory effect of hydrotalcite, IREC 2014 - 5th International Renewable Energy Congress (2014).

[40] A. Alejandre, F. Medina, X. Rodriguez, P. Salagre, Y. Cesteros, J.E. Sueiras, Cu/Ni/Al layered double hydroxides as precursors of catalysts for the wet air oxidation of phenol aqueous solutions, Appl. Catal. B: Environmental 30 (2001) 195–207.

[41] S. Kannan, V. Rives, H. Knözinger, High-temperature transformations of Cu-rich hydrotalcites, J. Solid State Chem. 177 (2004) 319–331. https://doi.org/10.1016/j.jssc.2003.08.023.

[42] Y. Ji, Z. Zhao, A. Duan, G. Jiang, J. Liu, Comparative Study on the Formation and Reduction of Bulk and Al2O3-Supported Cobalt Oxides by H2-TPR Technique, J. Phys. Chem. C. 113 (2009) 7186–7199. https://doi.org/10.1021/jp8107057.

[43] M. Śliwa, K. Samson, Influence of synthesis parameters on physicochemical properties of CuO/ZrO2 catalysts, Chem. Pap. 73 (2019) 2793–2802. https://doi.org/10.1007/s11696-019-00832-8.

[44] J. Cheng, J. Yu, X. Wang, L. Li, J. Li, Z. Hao, Novel CH 4 Combustion Catalysts Derived from Cu - Co/X - Al (X) Fe, Mn, La, Ce) Hydrotalcite-like Compounds, Energy Fuels 22 (2008) 2131–2137.

[45] J. Cheng, J. Yu, X. Wang, L. Li, J. Li, Z. Hao, Novel CH4 combustion catalysts derived from Cu-Co/X-Al (X = Fe, Mn, La, Ce) hydrotalcite-like compounds, Energy and Fuels. 22 (2008) 2131–2137. https://doi.org/10.1021/ef8000168.

[46] Z. Jiang, Z. Hao, J. Yu, H. Hou, C. Hu, J. Su, Catalytic combustion of methane on novel catalysts derived from Cu-Mg/Al-hydrotalcites, Catal. Letters. 99 (2005) 157–163. https://doi.org/10.1007/s10562-005-2108-6.

[47] F. QIN, Y. LIU, S. QING, X. HOU, Z. GAO, Cu-Al spinel as a sustained release catalyst for H2 production from methanol steam reforming: Effects of different copper sources, J. Fuel Chem. Technol. 45 (2017) 1481–1488. https://doi.org/https://doi.org/10.1016/S1872-5813(17)30065-8.

[48] H Dib, R. El Khawaja, G. Rochard, C. Poupin, S. Siffert, R. Cousin, CuAlCe Oxides Issued from Layered Double Total Oxidation, Catalysts, vol.10, issue 8, p 1-14 (2020).

[49] R. Xie, G. Fan, L. Yang, F. Li, Highly Efficient Hybrid Cobalt – Copper – Aluminum Layered Double Hydroxide / Graphene Nanocomposites as Catalysts for the Oxidation of Alkylaromatics, 100029 (2016) 363–371. https://doi.org/10.1002/cctc.201500890.

[50] M.C. Biesinger, Advanced analysis of copper X-ray photoelectron spectra, Surf. Interface Anal. 49 (2017) 1325–1334. https://doi.org/https://doi.org/10.1002/sia.6239.

[51] H.F. Wang, R. Kavanagh, Y.L. Guo, Y. Guo, G. Lu, P. Hu, Origin of extraordinarily high catalytic activity of Co3O 4 and its morphological chemistry for CO oxidation at low temperature, J. Catal. 296 (2012) 110–119. https://doi.org/10.1016/j.jcat.2012.09.005.

[52] M.J. Pollard, B.A. Weinstock, T.E. Bitterwolf, P.R. Griffiths, A. Piers Newbery, J.B. Paine, A mechanistic study of the low-temperature conversion of carbon monoxide to carbon dioxide over a cobalt oxide catalyst, J. Catal. 254 (2008) 218–225. https://doi.org/10.1016/j.jcat.2008.01.001.

[53] A. V. Salker, M.S.F. Desai, CO-NO/O2 redox reactions over Cu substituted cobalt oxide spinels, Catal. Commun. 87 (2016) 116–119. https://doi.org/10.1016/j.catcom.2016.09.016.

[54] M. Iwamoto, H. Hamada, Removal of nitrogen monoxide from exhaust gases through novel catalytic processes, Catal. Today. 10 (1991) 57–71.

[55] C.T. Goralski, W.F. Schneider, Analysis of the thermodynamic feasibility of NOx decomposition catalysis to meet next generation vehicle NOx emissions standards,

Appl. Catal. B Environ. 37 (2002) 263–277. https://doi.org/10.1016/S0926-3373(01)00317-4.

[56] G.C. Chinchen, M.S. Spencer, K.C. Waugh, D.A. Whan, Promotion of methanol synthesis and the water-gas shift reactions by adsorbed oxygen on supported copper catalysts, J. Chem. Soc. Faraday Trans. 1 Phys. Chem. Condens. Phases. 83 (1987) 2193–2212. https://doi.org/10.1039/F19878302193.

[57] Q.L. Tang, Z.X. Chen, X. He, A theoretical study of the water gas shift reaction mechanism on Cu(1 1 1) model system, Surf. Sci. 603 (2009) 2138–2144. https://doi.org/10.1016/j.susc.2009.04.011.

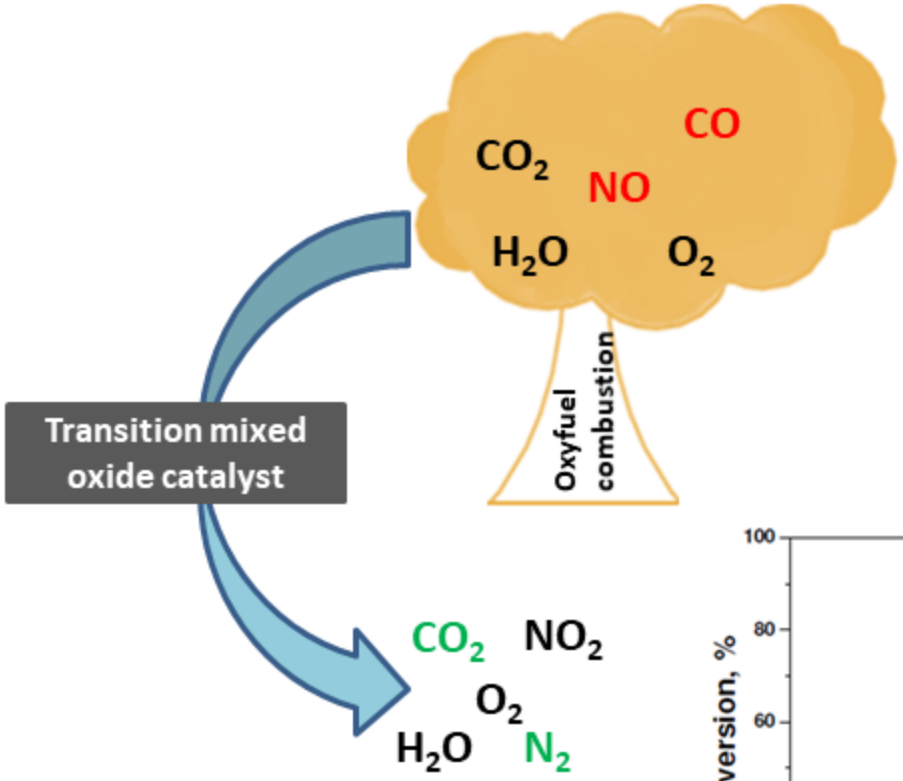

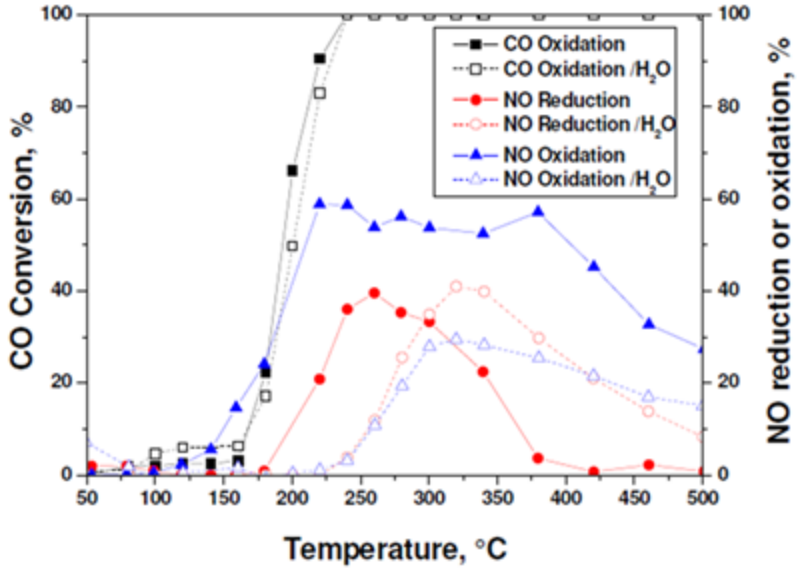

Conditions: 20% CO_2, 10% O_2, 0.5% CO, 0.02% NO and 8.2% H_2O in He